




ORIGINAL ARTICLE

Boron neutron capture therapy delays the decline in neurological function in a mouse model of metastatic spinal tumors

Yoshiki Fujikawa¹  | Shinji Kawabata¹  | Kohei Tsujino¹  | Hironori Yamada¹ | Hideki Kashiwagi¹  | Ryokichi Yagi¹ | Ryo Hiramatsu¹  | Naosuke Nonoguchi¹ | Toshihiro Takami¹ | Akinori Sasaki² | Naonori Hu²  | Takushi Takata³ | Hiroki Tanaka³  | Minoru Suzuki³ | Masahiko Wanibuchi¹ 

¹Department of Neurosurgery, Osaka Medical and Pharmaceutical University, Osaka, Japan

²Kansai BNCT Medical Center, Osaka Medical and Pharmaceutical University, Osaka, Japan

³Institute for Integrated Radiation and Nuclear Science, Kyoto University, Osaka, Japan

Correspondence

Shinji Kawabata, Department of Neurosurgery, Osaka Medical and Pharmaceutical University, 2-7 Daigakumachi, Takatsuki, Osaka 569-8686, Japan.
Email: shinji.kawabata@ompu.ac.jp

Funding information

Japan Society for the Promotion of Science, Grant/Award Number: JP22K09270 and JP23H03024

Abstract

Metastatic spinal tumors are increasingly prevalent due to advancements in cancer treatment, leading to prolonged survival rates. This rising prevalence highlights the need for developing more effective therapeutic approaches to address this malignancy. Boron neutron capture therapy (BNCT) offers a promising solution by delivering targeted doses to tumors while minimizing damage to normal tissue. In this study, we evaluated the efficacy and safety of BNCT as a potential therapeutic option for spine metastases in mouse models induced by A549 human lung adenocarcinoma cells. The animal models were randomly allocated into three groups: untreated ($n=10$), neutron irradiation only ($n=9$), and BNCT ($n=10$). Each mouse was administered 4-borono-L-phenylalanine (250 mg/kg) intravenously, followed by measurement of boron concentrations 2.5 h later. Overall survival, neurological function of the hindlimb, and any adverse events were assessed post irradiation. The tumor-to-normal spinal cord and blood boron concentration ratios were 3.6 and 2.9, respectively, with no significant difference observed between the normal and compressed spinal cord tissues. The BNCT group exhibited significantly prolonged survival rates compared with the other groups (vs. untreated, $p=0.0015$; vs. neutron-only, $p=0.0104$, log-rank test). Furthermore, the BNCT group demonstrated preserved neurological function relative to the other groups (vs. untreated, $p=0.0004$; vs. neutron-only, $p=0.0051$, multivariate analysis of variance). No adverse events were observed post irradiation. These findings indicate that BNCT holds promise as a novel treatment modality for metastatic spinal tumors.

Abbreviations: BBB, Basso–Beattie–Bresnahan; BNCT, boron neutron capture therapy; BPA, 4-borono-L-phenylalanine; CBE, compound biological effectiveness; CI, confidence interval; CT, computed tomography; D_B , boron dose; D_N , nitrogen dose; D_H , hydrogen dose; D_γ , gamma-ray dose; ESCC, epidural spinal cord compression; Gy-Eq, photon-equivalent dose; ICP-AES, inductively coupled plasma–atomic emission spectroscopy; KURNS, Kyoto University Institute for Integrated Radiation and Nuclear Science; LAT, L-type amino acid transporter; MANOVA, multivariate analysis of variance; MST, median survival time; QOL, quality of life; RBE, relative biological effectiveness; SF, surviving fraction; SBRT, stereotactic body radiation therapy; T/N, tumor-to-normal tissue ratio; T/BI, tumor-to-blood ratio.

This is an open access article under the terms of the [Creative Commons Attribution-NonCommercial](https://creativecommons.org/licenses/by-nc/4.0/) License, which permits use, distribution and reproduction in any medium, provided the original work is properly cited and is not used for commercial purposes.

© 2024 The Author(s). *Cancer Science* published by John Wiley & Sons Australia, Ltd on behalf of Japanese Cancer Association.

KEYWORDS

4-borono-L-phenylalanine, boron neutron capture therapy, neoplasm metastasis, spinal cord compression, spinal cord neoplasm

1 | INTRODUCTION

Boron neutron capture therapy (BNCT) is a unique cell-selective cancer treatment modality in which tumor cells are irradiated from within by high linear energy transfer particles emitted from the reaction of thermal neutrons with 10-boron atoms (^{10}B (n, α) ^7Li).¹ The released alpha particles and lithium recoil nuclei have a very short range (4–9 μm), depositing almost all their energy in the cells where the reaction occurs. Currently, 4-borono-L-phenylalanine (BPA) is the most widely used boron delivery agent for BNCT.^{2,3} Additionally, BPA predominantly infiltrates the cells through SLC7A5 (L-type amino acid transporter 1 [LAT1]), which is highly expressed in cancerous cells.^{4–6}

Metastatic spinal tumors frequently emerge as a secondary manifestation of distant recurrence in various solid cancers, including those originating from the lung, breast, and prostate.^{7,8} These metastatic lesions can induce epidural spinal cord compression (ESCC), leading to neurological deficits.⁹ Despite advancements in treatment options such as surgical interventions and modern radiation techniques like stereotactic body radiation therapy (SBRT), managing metastatic spinal tumors remains a formidable challenge.^{10,11} Furthermore, the palliative phase persists, emphasizing the urgent need for enhanced quality of life (QOL).

Numerous current clinical applications of BNCT for patients with malignancies, including glioblastoma, high-grade meningioma, head and neck cancers, and melanoma, have been documented.^{3,12–16} The use of accelerator-based neutron sources as medical devices for managing patients with cancer is already established in medical practice and is rapidly gaining popularity.^{15,17} However, to date, a notable lack of studies investigating the application of BNCT specifically for metastatic spinal tumors exists. Hence, this study aims to assess the efficacy and safety of BNCT using mouse models of metastatic spinal tumors.

2 | MATERIALS AND METHODS

2.1 | Cell culture

A549 human lung carcinoma cells were obtained from the ATCC (CCL-185™), while the U87MG human malignant glioma cells were generously provided by the Laboratory of Biological Macromolecules, Graduate School of Agriculture, Osaka Metropolitan University. A549 cells were selected for this study based on their relevance to non-small cell lung carcinoma, which represents the most common origin of metastatic spinal tumors and exhibits radioresistance.^{7,18} Additionally, U87MG cells were selected due to their association with glioblastoma, the target

malignancy in current clinical trials. Both cell lines were cultured in DMEM supplemented with 10% FBS, 100 U/mL penicillin, 100 $\mu\text{g}/\text{mL}$ streptomycin, and 250 ng/mL amphotericin B in a humidified incubator with 5% CO_2 atmosphere at 37°C. These culture materials were obtained from Gibco Invitrogen.

2.2 | Boron compound

^{10}B -enriched L-BPA was supplied by Interpharma Praha. The BPA-fructose complex was subsequently prepared as previously described.¹⁹ Moreover, the boron concentration was set to 1000 $\mu\text{g}/\text{mL}$.

2.3 | In vitro BPA uptake and clearance

A total of 2×10^5 A549 and U87MG cells were seeded in 100-mm dishes (Becton, Dickinson, and Company) and cultured for 5 days until reaching near-confluency. Subsequently, the BPA-containing medium was adjusted to a boron concentration of 10 $\mu\text{g}/\text{mL}$, and the cells were subsequently incubated for 2.5, 6, and 24 h. Additionally, after exposure to BPA for 24 h, the medium was replaced with a BPA-free medium, and the cells were further incubated for 1, 3, and 6 h. At each time point, the cells were rinsed with cold (4°C) PBS and detached using a trypsin-ethylenediamine tetra-acetic acid solution. After centrifugation at 1500 rpm for 5 min, the supernatant was removed, and the sedimented cells were stirred with PBS. This process was repeated twice. Subsequently, the collected cells were counted and digested overnight in 1 N nitric acid solution (Wako Pure Chemical Industries). The concentration of boron uptake was determined using inductively coupled plasma-atomic emission spectroscopy (ICP-AES; iCAP6300 emission spectrometer, Hitachi High-Technologies).

2.4 | Immunofluorescence

A549 and U87MG cells were seeded within individual chambers of a chamber slide (LAB-TEK®) and cultured for several days. The cells were fixed with 90% alcohol for 10 min, followed by treatment with PBS containing Tween-20 for 10 min at room temperature. Next, the primary antibody, human LAT1 polyclonal antibody (200 μL ; KE026, Trans Genic Inc.) was added to the cells at a dilution of 1:20 in Dako Antibody Diluent with Background Reducing Components (Dako) and incubated overnight at 4°C. The cells were then labeled with the secondary antibody, goat anti-rabbit IgG [H+L] (200 μL ; Alexa Fluor™ 488, A11034, Thermo Fisher Scientific Inc.), at a dilution

ratio of 1:200 for 2 h at room temperature in the dark. Between each step, the cells were rinsed thrice with PBS. Finally, the cells were stained with one drop of ibidi Mounting Medium with DAPI (ib50011; NIPPON Genetics Co, Ltd.) and observed using a confocal laser microscope (STELLARIS 8; Leica Microsystems GmbH).

2.5 | In vitro X-ray and neutron irradiation

Photon-equivalent biological effect ratios were calculated to compare the efficacy of photons and neutrons. In BNCT, the biological effect ratio, typically calculated as the compound biological effectiveness (CBE), considers the accumulation of boron compounds in target cells.

Photon-irradiation was performed at doses of 0, 2, 4, 6, and 8 Gy using a photon radiation device (M-150WE, SOFTEX, 2 mA, 100 kVp, dose rate 2.1 Gy/min) at room temperature. The cells were placed on the irradiation vessel, perpendicular to the direction of the photon beam (vertical beam). The irradiated cells were then seeded in 60-mm dishes (Becton, Dickinson, and Company) and cultured with a medium in 5% CO₂ atmosphere at 37°C for 7 days. Following incubation, the cells were fixed with 90% alcohol and stained with trypan blue (Gibco Invitrogen). The surviving fraction (SF) was determined by dividing the number of colonies by the number of colonies in the control group (0 Gy).

For the neutron irradiation experiment, cells were first preincubated in a medium either with or without 10 µg ¹⁰B/mL BPA for 24 h. Neutron irradiation was then conducted at a reactor power of 1 MW for 0, 10, 20, and 30 min at Kyoto University Institute for Integrated Radiation and Nuclear Science (KURNS). The subsequent procedures were identical to those described for photon irradiation. After obtaining the colony count, cell survival curves were generated. The biological endpoint for determining the CBE factor of BPA for the A549 cells was set at SF 0.1.

2.6 | Animal model preparation

Eight-week-old male BALB/c nude mice were purchased from Japan SLC, Inc. The mice were housed in standard facilities with no more than five mice per cage, with food and water available ad libitum. The temperature was maintained at 21 ± 2°C, and lighting adhered to a strict 12-h/12-h light-dark cycle. In addition, after the tumor-bearing models were established and a decline in neurological function was observed, manual pressure was applied to the lower abdomen once daily to induce urination.

A549 cells were suspended in serum-free DMEM/1.3% agarose (Wako Pure Chemical Industries) mixture (1:1) at a concentration of 2 × 10⁶ cells per 200 µL. The cell suspension was then subcutaneously injected into the right flank of each mouse. After 7–10 days, the subcutaneous tumors were harvested, submerged in cold PBS, and maintained on ice until they were ready to be implanted into the mouse spine.

This study was performed in accordance with both the Guide for the Care and Use of Laboratory Animals and the Declaration of Helsinki. Approval was granted by the Animal Use Review Board of Osaka Medical and Pharmaceutical University (approval no. AM2023-019) and the Ethical Committee of KURNS (approval no. R5031).

2.7 | Animal surgery

The surgical procedure was performed following a protocol similar to that highlighted in a previous report.²⁰ In brief, after intraperitoneal injection of anesthesia with medetomidine (0.4 mg/kg; ZENOAQ), midazolam (2.0 mg/kg; SANDOZ), and butorphanol (5.0 mg/kg; Meiji Seika), surgery was performed under a desktop microscope (Olympus). A 2 cm wide skin incision was made using a scalpel, and the underlying dorsal muscles were bilaterally stripped to expose the spinous process and lamina at two levels. The spinous processes were removed using rongeurs, and the lamina was decorticated using a hand drill. A 5 mm³ piece of the harvested tumor was positioned onto the decorticated area and the muscle fascia was tightly sutured using 4-0 nylon sutures. Finally, the skin was closed separately.

2.8 | Histopathological image

Upon development of paraplegia in the metastatic spinal tumor model mice, the mice were euthanized, and samples of the tumor and tissues were harvested. These samples were then fixed in 10% formalin for 24 h. Subsequently, the samples were embedded in paraffin (Nara-byouri Laboratory Co., Ltd.), sectioned into 3-µm slices, and stained with H&E (Muto Pure Chemicals Co., Ltd.).

2.9 | Biodistribution of BPA

A549 spinal metastatic tumor model mice were administered BPA at a dose of 250 mg/kg via the tail vein after they developed paraparesis. Next, the mice were divided into three groups (*n* = 3 in each group). Following the BPA administration for either 2.5, 6, or 24 h, the mice in each respective group were euthanized. Various tissues, including the tumor, compressed spinal cord, normal spinal cord, blood, liver, kidney, and small intestine, were then harvested. These samples were soaked in 1 N nitric acid solution for 7 days, after which the boron concentration was measured using ICP-AES.

2.10 | In vivo BNCT experiments

Thirty spinal metastatic tumor models were established for the in vivo neutron irradiation experiment. Unfortunately, one mouse succumbed to anesthetic-related complications, resulting in a total

of 29 mice available for analysis. These mice were randomly assigned to three groups: the untreated ($n=10$), the neutron-only ($n=9$), and the BNCT group ($n=10$). Neutron irradiation was conducted 21 days after tumor implantation at the heavy water facility of KURNS at a reactor power of 5 MW for 10 min.

In the BNCT group, BPA (250 mg/kg) was injected intravenously 2.5 h before irradiation. Mice in both irradiated groups were intraperitoneally anesthetized and confined within an acrylic cage during irradiation. Each mouse's body, except for the tumor-implanted area, was shielded by a plate lined with ^6LiF ceramic tiles to mitigate radiation exposure.

Overall survival was investigated, and the percent increase in life span was calculated using the following formula: $(\text{MST of each irradiation group} - \text{MST of the untreated group}) \times 100 / \text{MST of the untreated group}$ (MST, median survival time). Furthermore, the neurological function of the hindlimb of each mouse was evaluated using the Basso–Beattie–Bresnahan (BBB) score,²¹ which ranges from 21 (normal function) to 0 (complete paraplegia). The BBB score for each group was recorded two to three times per week and averaged. The experimental endpoint was defined as a BBB score ≤ 7 (indicating paraplegia and hindlimb sweeping) or a body weight loss of $\geq 20\%$. After the mice were euthanized, we histopathologically examined the small intestine, kidney, liver, and spinal cord of each group.

2.11 | Computed tomography (CT)

Before CT imaging using the LCT-200 series (Hitachi) with the tube power voltage and current set at 50 kV and 0.5 mA, respectively, the tumor-bearing mice were anesthetized and intravenously administered a contrast agent at a dose of 20 mg/kg. The voxel size was $48 \times 48 \mu\text{m}$, and the thickness of each image slice was $192 \mu\text{m}$.

2.12 | Dosimetry

Thermal neutron flux during neutron irradiation was measured using the radioactivity of gold foils ($50 \mu\text{m}$ thick, 3 mm diameter) attached to the upstream and downstream of the tube containing cell suspension (in vitro), as well as the ventral and dorsal surface of the mice (in vivo). The mice were irradiated from the ventral side for stability during irradiation. Gamma-ray doses were also measured using a thermoluminescence dosimeter.

The total absorbed dose of BNCT includes boron (D_B), nitrogen (D_N), hydrogen (D_H), and gamma-ray doses (D_γ). The photon-equivalent dose (Gy-Eq) was determined using the following formula: $D_B \times \text{CBE} + D_N \times \text{relative biological effectiveness of nitrogen (RBE}_N) + D_H \times \text{RBE of hydrogen (RBE}_H) + D_\gamma \times \text{RBE of gamma-ray (RBE}_\gamma)$.²²

The CBE was set at 1.35, 4.9, and 4.25 for the spinal cord, small intestine, and liver, respectively.^{23–26} The CBE for the tumor was determined from the result of the in vitro study. The RBE_N and RBE_H were both set at 3.0, while the RBE_γ was 1.0.²⁷ The D_B was calculated from the results of the biodistribution study. The photon-equivalent dose for various organs was calculated using CT images, applying conversion factors specific to each organ based on measurements from the gold foil on the ventral side. From these calculated doses and CT images, two-dimensional dose distributions were created.

2.13 | Data analysis

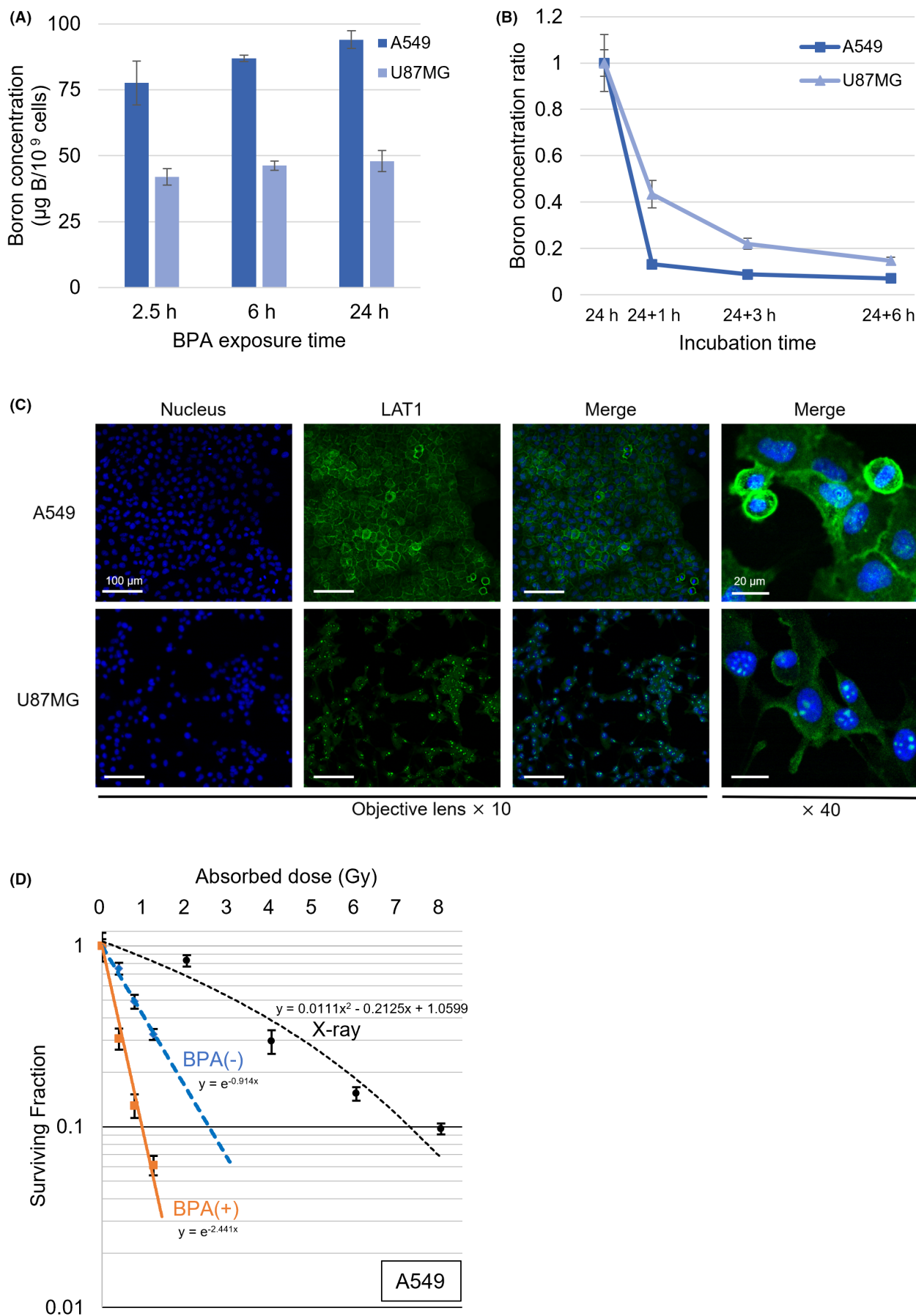
Statistical analysis was performed using JMP® Pro 16.2.0 software (SAS Institute). Differences in the in vitro data were assessed using Student's *t*-test. Overall survival was summarized as the mean and median number of days with 95% confidence intervals (CI) and evaluated using Kaplan–Meier curves. The significance of survival duration was analyzed using the log-rank test. Moreover, the average BBB score of each group was plotted to illustrate neurological function after BNCT, and multivariate analysis of variance (MANOVA) was employed. Any missing values were substituted with the most recent observations. A *p*-value < 0.05 was considered statistically significant.

3 | RESULTS

3.1 | In vitro BPA uptake and clearance

A549 cells exhibited a higher BPA uptake after 24 h compared with that after 2.5 h ($p=0.02$, Student's *t*-test). No significant differences were observed among the other combinations of time points. In U87MG cells, no significant differences were observed in BPA uptake across the various time points (Figure 1A). In comparison with U87MG cells, A549 cells exhibited a faster reduction in boron clearance upon switching to a BPA-free medium. The boron concentration decreased by 13.2% in A549 cells and by 43.4% in U87MG cells after 1 h of incubation ($p < 0.0001$ for both; Figure 1B).

FIGURE 1 (A) In vitro 4-borono-L-phenylalanine (BPA) uptake. Both A549 and U87MG cells were treated with $10 \mu\text{g B/mL}$ of BPA for 2.5, 6, and 24 h. In A549 cells, the boron concentration at 24 h is significantly higher than that at 2.5 h ($p=0.02$, Student's *t*-test). In U87MG cells, the BPA uptake did not differ across each time point. (B) After 24 h exposure to BPA, the cells were incubated with a BPA-free medium for an additional 1, 3, or 6 h. Data are expressed as the mean \pm SD. (C) Immunofluorescence images of L-amino acid transporter (LAT) 1. A549 cells markedly expressed LAT1 on the cell membrane compared with its expression in U87MG cells. Scale bar = 100 and $20 \mu\text{m}$ for objective lens $\times 10$, and $\times 40$, respectively. (D) Survival lines and curve of A549 cells irradiated with neutrons and photons. Neutron irradiation is conducted for 0, 10, 20, and 30 min with or without BPA. The corresponding absorbed doses are 0.40, 0.77, and 1.2 Gy for 10, 20, and 30 min, respectively. Error bars represent SD.



3.2 | Immunofluorescence

The expression of LAT1 was predominantly observed on the cell membrane of A549 cells. In contrast, the U87MG cells exhibited a relatively low expression of LAT1. The internalization of LAT1 expression from the cell surface was more pronounced compared with that observed in A549 cells (Figure 1C).

3.3 | In vitro X-ray and neutron irradiation

Figure 1D displays the SF of A549 cells following photon and neutron irradiation. The average thermal neutron flux was 1.75×10^9 neutrons/cm²/s. The details of each dose and dose rate are shown

in Table 1. Neutron irradiation, particularly in conjunction with BPA exposure, demonstrated a stronger cell-killing effect than that exhibited by photon irradiation. When the SF reached 0.1, the photon dose was 7.3 Gy, the total dose without BPA was 2.52 Gy, and the total dose with BPA was 0.94 Gy. Based on these findings, the CBE factor of BPA for A549 cells was calculated to be 2.12.

3.4 | Histopathological image

The histological images obtained revealed established tumors severely compressing the spinal cord from the epidural space. Certain sections of the compressed spinal cord exhibited a spongy appearance (Figure 2A).

TABLE 1 Details of each dose and dose rate in the in vitro neutron irradiation.

	Boron dose (Gy)	Nitrogen dose (Gy)	Hydrogen dose (Gy)	Gamma-ray (Gy)
10min	0.094	0.19	0.11	0.10
20min	0.17	0.35	0.20	0.22
30min	0.28	0.55	0.31	0.35
Average dose rate \pm SD (Gy/min)	0.0091 ± 0.00036	0.018 ± 0.00072	0.010 ± 0.00041	0.011 ± 0.00074

FIGURE 2 (A) Histopathological images stained with H&E reveal epidural spinal cord compression (yellow dotted line) caused by the tumor mass (white dotted line). Degenerative and congestive changes are observed in the compressed spinal cord (magnified image). (B) Biodistribution of boron in the mouse metastatic spinal tumor model. The boron concentration is measured after intravenous administration of 4-borono-L-phenylalanine (BPA; 250 mg/kg) at each time point ($n=3$). Data are displayed as the mean \pm SD. SC, spinal cord; Tu, tumor; VB, vertebral body.

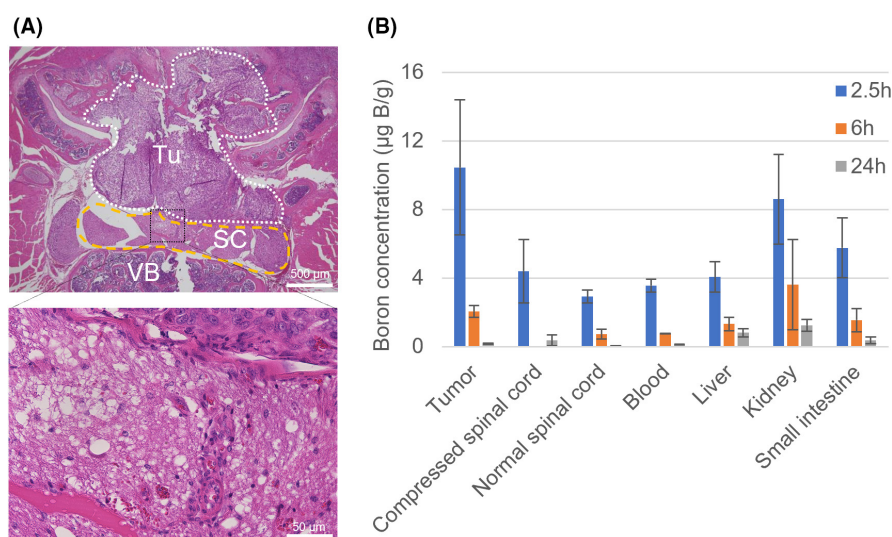
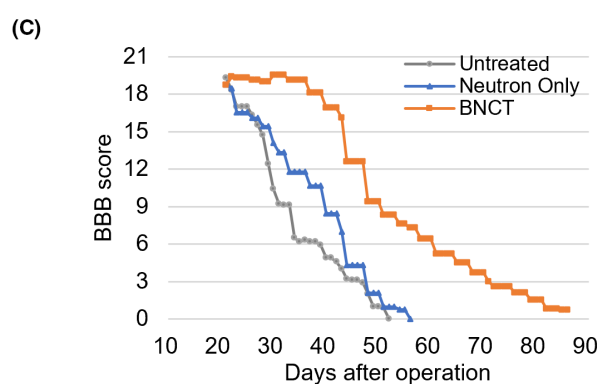
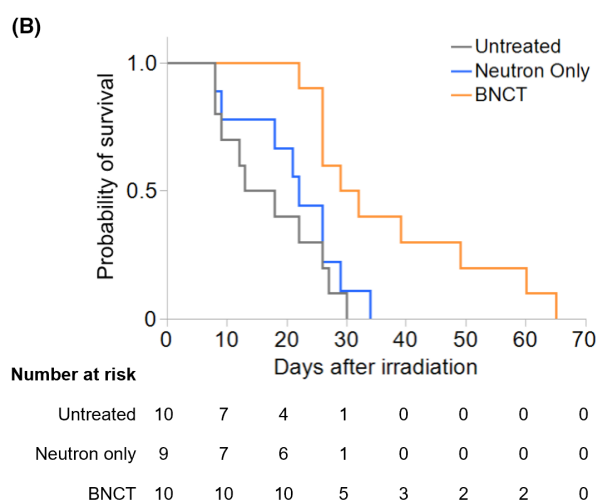
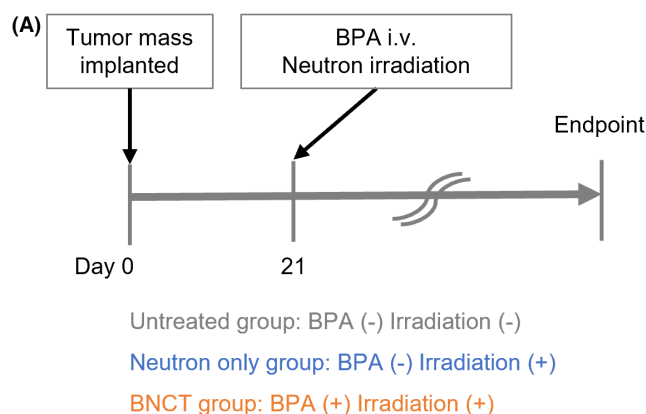


TABLE 2 Biodistribution of boron and ratios.

Time	n	Boron concentration \pm SD (μ g B/g) ^a							Ratio	
		Tumor	Compressed spinal cord	Normal spinal cord	Blood	Liver	Kidney	Small intestine	T/N	T/BI
2.5h	3	10.5 \pm 3.9	4.4 \pm 1.9	2.9 \pm 0.37	3.6 \pm 0.37	4.06 \pm 0.88	8.6 \pm 2.6	5.8 \pm 1.7	3.6	2.9
6h	3	2.05 \pm 0.35	N/A	0.75 \pm 0.28	0.75 \pm 0.0095	1.32 \pm 0.38	3.6 \pm 2.6	1.6 \pm 0.67	2.8	2.7
24h	3	0.18 \pm 0.031	0.37 \pm 0.31	0.038 \pm 0.016	0.14 \pm 0.017	0.81 \pm 0.24	1.2 \pm 0.34	0.36 \pm 0.19	4.7	1.3

Abbreviations: T/BI, tumor-to-blood ratio; T/N, tumor-to-normal spinal cord ratio.

^aData are expressed as the mean \pm SD.



3.5 | Biodistribution of BPA

The boron concentration of the tumors and organs peaked at 2.5 h after BPA administration (Figure 2B). The tumor-to-normal spinal cord ratio (T/N) and tumor-to-blood ratio (T/B) at 2.5 h were both approximately 3.0 (Table 2). In addition, the boron concentration of the compressed spinal cord adjacent to the tumor was assessed, and no significant difference was identified compared with that of the normal spinal cord at 2.5 h ($p=0.33$, Student's *t*-test).

FIGURE 3 The in vivo boron neutron capture therapy (BNCT) experiments. (A) The experimental protocol from surgery (day 0), through neutron irradiation with or without intravenous 4-borono-L-phenylalanine (BPA; day 21), to the endpoint. The mice are randomly assigned to untreated ($n=10$), neutron-only ($n=9$), or BNCT groups ($n=10$). (B) The Kaplan-Meier survival curve and mice at risk. The BNCT group exhibits a significantly prolonged survival compared with the other groups (vs. untreated group, $p<0.01$; vs. neutron-only group, $p<0.05$, log-rank test). (C) Neurological function is assessed by the Basso-Beattie-Bresnahan (BBB) score. Statistically significant differences are identified in the BNCT group compared with those in the other groups (vs. untreated group, $p<0.001$; vs. neutron-only group, $p<0.01$, multivariate analysis of variance). Data are displayed as the mean.

3.6 | In vivo BNCT experiments

According to the biodistribution study, BPA was administered 2.5 h before neutron irradiation. The experimental procedure is illustrated in Figure 3A. Kaplan-Meier analysis revealed a significant prolongation of survival in the BNCT group compared with that in the other groups (vs. untreated, $p=0.0015$; vs. neutron-only, $p=0.0104$, respectively, log-rank test). No significant survival benefit was observed in the neutron-only group compared with the untreated group (Figure 3B). The MST of the untreated or neutron-only group was approximately 40 days, whereas that of the BNCT group was 52 days (Table 3).

A significant improvement in neurological function was observed in the BNCT group compared with that in the other groups (vs. untreated, $p=0.0004$; vs. neutron-only, $p=0.0051$, respectively, MANOVA). However, no significant difference was observed between the untreated and neutron-only groups ($p=0.26$; Figure 3C).

Table 4 demonstrates the radiation doses, measured as both the absorbed dose and the Gy-Eq, which were delivered to the tumors and surrounding tissues within the irradiation field. The average thermal neutron flux at the ventral side was 5.95×10^9 neutrons/cm²/s. The photon-equivalent dose to the tumor was almost 3 Gy-Eq, while the dose to the spinal cord was about half of that delivered to the tumor. In contrast, the small intestine received an equivalent dose exceeding 8 Gy-Eq. The distribution of equivalent doses is illustrated in two-dimensional representations (Figure 4A).

Furthermore, no noticeable adverse radiation effects such as paralysis before tumor enlargement (attributable to radiation myelopathy), diarrhea, or intestinal bleeding were observed. Histopathological examination after irradiation revealed no significant differences in any of the organs among the groups (Figure 4B).

4 | DISCUSSION

In this pilot study, we have demonstrated that BNCT using BPA prolonged survival and preserved neurological function in mouse models of metastatic spinal tumors. Furthermore, no radiotoxicities were observed after neutron irradiation. To the best of our knowledge,

TABLE 3 Overall survival of the metastatic spinal tumor models.

Group	n	Overall survival (days)			%ILS ^a	p-Value ^b	
		Mean \pm SD	Median	95% CI		vs. Untreated	vs. Neutron only
Untreated	10	38 \pm 8	37	29–47	–	–	–
Neutron-only	9	42 \pm 8	43	29–50	8.2	0.39	–
BNCT	10	58 \pm 15	52	43–70	41.1	0.0015	0.0104

Abbreviations: BNCT, boron neutron capture therapy; CI, confidence interval; ILS, increase in life span; MST, median survival time.

^a%ILS was determined using the following formula: $(\text{MST of each irradiated group} - \text{MST of the untreated control group}) \times 100 / \text{MST of the untreated control group}$.

^bWe used the log-rank test to calculate p-values.

TABLE 4 The absorbed and photon-equivalent doses to the tumors and normal tissues of each group.

Group	Absorbed dose ^a (Gy)				Photon-equivalent dose ^b (Gy-Eq)			
	Liver	Small intestine	Spinal cord	Tumor	Liver	Small intestine	Spinal cord	Tumor
Untreated	–	–	–	–	–	–	–	–
Neutron only	1.08	1.69	0.74	0.74	2.01	3.22	1.35	1.35
BNCT	1.45	2.80	1.07	1.51	3.59	8.68	1.74	2.81

Abbreviation: BNCT, boron neutron capture therapy.

^aThe absorbed doses were calculated using the following formula: $D_B + D_N + D_H + D_\gamma$, where D_B , boron dose; D_N , nitrogen dose; D_H , hydrogen dose; D_γ , gamma-ray dose.

^bThe photon-equivalent doses were calculated using the following formula: $D_B \times \text{compound biological effectiveness (CBE)} + D_N \times \text{relative biological effectiveness of nitrogen (RBE}_N) + D_H \times \text{RBE of hydrogen (RBE}_H) + D_\gamma \times \text{RBE of gamma-ray (RBE}_\gamma)$. The CBE factors of 4-borono-L-phenylalanine (BPA) for the liver, small intestine, spinal cord, and tumor were set at 4.25, 4.9, 1.35, and 2.12, respectively. The values of RBE_N and RBE_H were both 3.0, and RBE_γ was 1.0.

this is the first in vivo experimental study focusing on BNCT for metastatic spinal tumors.

The survival rate of X-ray-irradiated A549 cells was consistent with the rate in the previous literature, indicating their radioresistant nature.²⁸ Additionally, immunofluorescence images displayed a higher expression of LAT1 on the cell membranes of A549 cells compared with that in the U87MG cells. This result may be associated with the difference in BPA uptake and clearance between A549 and U87MG cells. The high expression of LAT1 at the cell membrane may indicate an activated state, while the internalization of LAT1 from the cell membrane may be induced by down-regulation,²⁹ resulting in differences in both accumulation and clearance of BPA. This underscores the validity of the established clinical practice of administering a continuous intravenous infusion of BPA during irradiation.^{15,17} For cancers characterized by high LAT1 expression, particularly those that are radioresistant, BNCT using BPA may offer an effective and promising therapeutic strategy.

In the in vivo study, we employed metastatic spinal tumor models characterized by hindlimb paresis induced by ESCC. In contrast to previous studies focusing on the effects of BNCT on the normal spinal cord, our study specifically evaluated the compressed spinal cord affected by tumor progression.^{22,30} Moreover, ESCC is a serious complication that affects approximately 10% of patients

with spine metastases. The condition can lead to gait disturbances, severely impacting QOL, often necessitating urgent interventions such as decompressive surgery.^{8,9,31} As demonstrated in our representative histopathological image, previous animal studies have displayed that ESCC is correlated with white matter edema and axonal swelling, potentially resulting in white matter necrosis and gliosis.^{32,33} Therefore, concerns arose regarding potential alterations in the biodistribution of boron; however, our findings revealed no significant difference in BPA accumulation between the compressed and normal spinal cord. Furthermore, the T/N ratios exceeded 3.0, indicating favorable conditions for conducting BNCT in this animal model.³⁴

In this in vivo BNCT study, our results were favorable, aligning with expectations from in vitro and biodistribution studies. Furthermore, no apparent adverse events were observed, which may be supported by histopathological findings. As the mice were irradiated from the ventral side, the absorbed dose to the tumor, located dorsally, was relatively low. On the other hand, the small intestine, considered one of the organs at risk, exhibited a higher equivalent dose than that displayed by the other organs. However, no evidence of histopathological changes was present at this dose. This study demonstrated the safety of BNCT while highlighting the challenges of deep lesions. If we had irradiated the mice from the dorsal side, the result might have been much different.

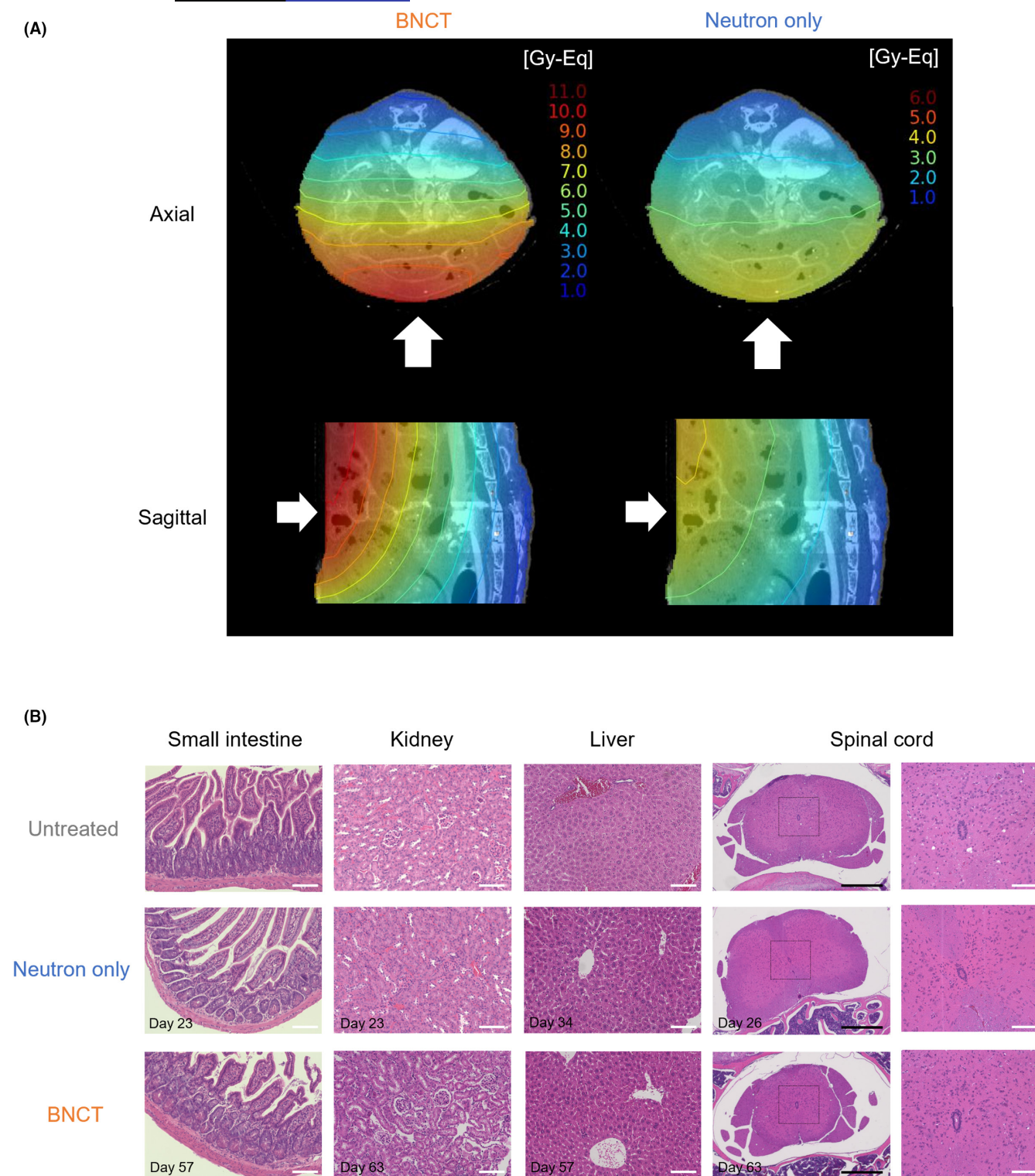


FIGURE 4 (A) Two-dimensional distributions of the equivalent radiation doses delivered to the tumor-bearing mice in the boron neutron capture therapy (BNCT) and neutron-only groups. White arrows indicate the direction of neutron irradiation. (B) Histological images of the small intestine, kidney, liver, and spinal cord of each group. Tissue sections are stained using H&E. No significant differences were observed in any of the tissues among the groups. Scale bars=100 (white) and 500 (black) μm. Day in each image represents the number of days after irradiation.

Radiotherapy and surgery stand as the principal treatment options for metastatic spinal tumors. Notably, over the past decade, SBRT has advanced the objectives of effective palliation

compared with conventional external-beam radiation therapy.^{35,36} The incidence of radiation myelopathy has been reported to be very low in the SBRT setting.¹¹ Nonetheless, SBRT is not exempt

from limitations. The risk of neurological deterioration after SBRT, especially for tumors causing high-grade ESCC, and in cases of re-irradiation, curtails its widespread use in preventing radiation myelopathy.^{11,37} Moreover, a previous study reported that 16% of patients with epidural compression of radioresistant cancers experienced a neurological decline after radiosurgery.³⁸

To deliver safe SBRT, patients with high-grade ESCC frequently undergo a tumor reduction procedure referred to as “separation surgery,” which establishes a 1–2-mm margin between the spinal cord and the tumor that is in direct contact with it.³⁹ In addition, with patients with cancer experiencing prolonged lifespans due to recent advances in cancer therapies, increased attention is needed regarding delayed adverse radiation effects following SBRT. A retrospective study conducted at a single institution revealed that the actuarial 10-year rate of late toxicity after SBRT was 17% in patients with spine metastases.⁴⁰

Boron neutron capture therapy offers the potential to selectively eliminate cancer cells while sparing normal cells in a single treatment session.²² This technique leverages the selective accumulation of boron-10 in tumor cells over that in adjacent normal cells, enabling targeted treatment at the microscopic level. These advantages of BNCT may eliminate the need for separation surgery for patients with high-grade ESCC.

Additionally, BNCT can administer potent doses directly to tumors while minimizing exposure to surrounding healthy tissue. This attribute makes BNCT a viable option even for patients previously subjected to radiotherapy, offering hope to those with cancers that are difficult to treat using conventional therapies. However, an essential consideration is the attenuation of neutron beams, as they penetrate deep into the body.⁴¹ This factor must be carefully considered when planning BNCT treatments, particularly because the spinal column, positioned at a certain depth beneath the skin, typically falls within the effective range for neutron irradiation. This emphasizes the promising potential of BNCT in addressing the aforementioned condition.

The study has a few limitations. First, due to scheduling constraints, the *in vivo* BNCT study was conducted for a pre-determined duration of 10min, rather than being based on the irradiation time determined by dose-limiting tissue. Further studies should include more detailed dose planning to address this limitation. Second, we performed *in vivo* neutron irradiation before neurological deterioration was evident (with an average BBB score of 19 for each group), indicating that the tumor did not severely compress the spinal cord. To confirm the efficacy of BNCT for spinal metastases with high-grade ESCC, neutron irradiation needs to be delayed until the onset of neurological deterioration in future studies. Third, tumor-bearing mice were implanted in the posterior lamina, whereas clinically, metastatic spinal tumors are more commonly observed in the vertebral body rather than in the lamina. Therefore, the impact of BNCT on spine metastases might vary depending on the location of the tumor. Finally, although no histopathological changes were observed among groups, caution

should be exercised because the timing of the tissue harvest was different.

In conclusion, our study demonstrates the efficacy and safety of *in vivo* BNCT using metastatic spinal tumor models derived from lung cancer cells. These findings suggest that BNCT holds promise as an effective and safe treatment option for metastatic spinal tumors. Further research is warranted to strengthen the evidence supporting the potential therapeutic benefits of BNCT for this disease and to facilitate its translation into clinical practice.

AUTHOR CONTRIBUTIONS

Yoshiki Fujikawa: Data curation; formal analysis; investigation; methodology; validation; visualization; writing – original draft. **Shinji Kawabata:** Conceptualization; funding acquisition; project administration; validation; writing – review and editing. **Kohei Tsujino:** Methodology. **Hironori Yamada:** Methodology. **Hideki Kashiwagi:** Methodology. **Ryokichi Yagi:** Methodology. **Ryo Hiramatsu:** Methodology. **Naosuke Nonoguchi:** Methodology. **Toshihiro Takami:** Funding acquisition. **Akinori Sasaki:** Resources. **Naonori Hu:** Resources. **Takushi Takata:** Formal analysis; visualization. **Hiroki Tanaka:** Resources. **Minoru Suzuki:** Resources. **Masahiko Wanibuchi:** Supervision.

ACKNOWLEDGMENTS

The authors would like to thank Aya Sunamura for her secretarial work and Itsuko Inoue, Nobuo Takasu, and Yuri Omori for their technical assistance.

FUNDING INFORMATION

This research was funded by the Japan Society for the Promotion of Science (JSPS) KAKENHI, grant number JP22K09270 to Toshihiro Takami (Grants-in-Aid for Science Research [C]) and partly by JP23H03024 to Shinji Kawabata (Grants-in-Aid for Science Research [B]).

CONFLICT OF INTEREST STATEMENT

The authors have no conflict of interest.

ETHICS STATEMENTS

Approval of the research protocol by an Institutional Reviewer Board: N/A.

Informed Consent: N/A.

Registry and the Registration No. of the study/trial: N/A.

Animal Studies: This study was approved by the Animal Use Review Board and the Ethical Committee of Osaka Medical and Pharmaceutical University (Approval No. AM2023-019) and KURNS (Approval No. R5031).

ORCID

Yoshiki Fujikawa  <https://orcid.org/0000-0002-7672-9266>

Shinji Kawabata  <https://orcid.org/0000-0001-5007-5279>

Kohei Tsujino  <https://orcid.org/0000-0002-2274-3214>

Hideki Kashiwagi  <https://orcid.org/0000-0003-3192-4065>

Ryo Hiramatsu  <https://orcid.org/0000-0002-5581-5472>

Naonori Hu  <https://orcid.org/0000-0003-2702-3344>

Hiroki Tanaka  <https://orcid.org/0000-0002-6195-3177>

Masahiko Wanibuchi  <https://orcid.org/0000-0002-1856-7123>

REFERENCES

- Barth RF, Grecula JC. Boron neutron capture therapy at the crossroads - where do we go from here? *Appl Radiat Isot*. 2020;160:109029.
- Mishima Y, Honda C, Ichihashi M, et al. Treatment of malignant melanoma by single thermal neutron capture therapy with melanoma-seeking 10B-compound. *Lancet*. 1989;2:388-389.
- Barth RF, Vicente MG, Harling OK, et al. Current status of boron neutron capture therapy of high grade gliomas and recurrent head and neck cancer. *Radiat Oncol*. 2012;7:146.
- Detta A, Cruickshank GS. L-amino acid transporter-1 and boronophenylalanine-based boron neutron capture therapy of human brain tumors. *Cancer Res*. 2009;69:2126-2132.
- Wongthai P, Hagiwara K, Miyoshi Y, et al. Boronophenylalanine, a boron delivery agent for boron neutron capture therapy, is transported by ATB0+, LAT1 and LAT2. *Cancer Sci*. 2015;106:279-286.
- Yoshimoto M, Honda N, Kurihara H, et al. Non-invasive estimation of (10) B-4-borono-L-phenylalanine-derived boron concentration in tumors by PET using 4-borono-2-(18) F-fluoro-phenylalanine. *Cancer Sci*. 2018;109:1617-1626.
- Wewel JT, O'Toole JE. Epidemiology of spinal cord and column tumors. *Neurooncol Pract*. 2020;7:i5-i9.
- Van den Brande R, Cornips EM, Peeters M, Ost P, Billiet C, Van de Kelft E. Epidemiology of spinal metastases, metastatic epidural spinal cord compression and pathologic vertebral compression fractures in patients with solid tumors: a systematic review. *J Bone Oncol*. 2022;35:100446.
- Rades D, Abraham JL. The role of radiotherapy for metastatic epidural spinal cord compression. *Nat Rev Clin Oncol*. 2010;7:590-598.
- Laufer I, Bilsky MH. Advances in the treatment of metastatic spine tumors: the future is not what it used to be. *J Neurosurg Spine*. 2019;30:299-307.
- Guckenberger M, Dahele M, Ong WL, Sahgal A. Stereotactic body radiation therapy for spinal metastases: benefits and limitations. *Semin Radiat Oncol*. 2023;33:159-171.
- Malouff TD, Seneviratne DS, Ebner DK, et al. Boron neutron capture therapy: a review of clinical applications. *Front Oncol*. 2021;11:601820.
- Matsumura A, Asano T, Hirose K, Igaki H, Kawabata S, Kumada H. Initiatives toward clinical boron neutron capture therapy in Japan. *Cancer Biother Radiopharm*. 2023;38:201-207.
- Takai S, Wanibuchi M, Kawabata S, et al. Reactor-based boron neutron capture therapy for 44 cases of recurrent and refractory high-grade meningiomas with long-term follow-up. *Neuro Oncol*. 2022;24:90-98.
- Hirose K, Konno A, Hiratsuka J, et al. Boron neutron capture therapy using cyclotron-based epithermal neutron source and borofalan ((10)B) for recurrent or locally advanced head and neck cancer (JHN002): an open-label phase II trial. *Radiother Oncol*. 2021;155:182-187.
- Hiratsuka J, Kamitani N, Tanaka R, et al. Long-term outcome of cutaneous melanoma patients treated with boron neutron capture therapy (BNCT). *J Radiat Res*. 2020;61:945-951.
- Kawabata S, Suzuki M, Hirose K, et al. Accelerator-based BNCT for patients with recurrent glioblastoma: a multicenter phase II study. *Neurooncol Adv*. 2021;3:vdb067.
- Barzilai O, Boriani S, Fisher CG, et al. Essential concepts for the Management of Metastatic Spine Disease: what the surgeon should know and practice. *Global Spine J*. 2019;9:98s-107s.
- Coderre JA, Button TM, Micca PL, Fisher CD, Nawrocky MM, Liu HB. Neutron capture therapy of the 9L rat gliosarcoma using the p-boronophenylalanine-fructose complex. *Int J Radiat Oncol Biol Phys*. 1994;30:643-652.
- Wang L, Rahman S, Lin CY, et al. A novel murine model of human renal cell carcinoma spinal metastasis. *J Clin Neurosci*. 2012;19:881-883.
- Basso DM, Beattie MS, Bresnahan JC. A sensitive and reliable locomotor rating scale for open field testing in rats. *J Neurotrauma*. 1995;12:1-21.
- Coderre JA, Morris GM. The radiation biology of boron neutron capture therapy. *Radiat Res*. 1999;151:1-18.
- Fukuda H. Response of normal tissues to boron neutron capture therapy (BNCT) with (10)B-Borocaptate sodium (BSH) and (10)B-Paraboronophenylalanine (BPA). *Cells*. 2021;10:2883.
- Morris GM, Coderre JA, Hopewell JW, et al. Response of the central nervous system to boron neutron capture irradiation: evaluation using rat spinal cord model. *Radiother Oncol*. 1994;32:249-255.
- Coderre JA, Morris GM, Kalef-Ezra J, et al. The effects of boron neutron capture irradiation on oral mucosa: evaluation using a rat tongue model. *Radiat Res*. 1999;152:113-118.
- Suzuki M, Masunaga SI, Kinashi Y, et al. The effects of boron neutron capture therapy on liver tumors and normal hepatocytes in mice. *Jpn J Cancer Res*. 2000;91:1058-1064.
- Suzuki M, Kato I, Aihara T, et al. Boron neutron capture therapy outcomes for advanced or recurrent head and neck cancer. *J Radiat Res*. 2014;55:146-153.
- Dong JC, Gao H, Zuo SY, et al. Neuropilin 1 expression correlates with the radio-resistance of human non-small-cell lung cancer cells. *J Cell Mol Med*. 2015;19:2286-2295.
- Ohno Y, Suda K, Masuko K, Yagi H, Hashimoto Y, Masuko T. Production and characterization of highly tumor-specific rat monoclonal antibodies recognizing the extracellular domain of human L-type amino-acid transporter 1. *Cancer Sci*. 2008;99:1000-1007.
- Morris GM, Coderre JA, Micca PL, Fisher CD, Capala J, Hopewell JW. Central nervous system tolerance to boron neutron capture therapy with p-boronophenylalanine. *Br J Cancer*. 1997;76:1623-1629.
- Patchell RA, Tibbs PA, Regine WF, et al. Direct decompressive surgical resection in the treatment of spinal cord compression caused by metastatic cancer: a randomised trial. *Lancet*. 2005;366:643-648.
- Kato A, Ushio Y, Hayakawa T, Yamada K, Ikeda H, Mogami H. Circulatory disturbance of the spinal cord with epidural neoplasm in rats. *J Neurosurg*. 1985;63:260-265.
- Manabe S, Tanaka H, Higo Y, Park P, Ohno T, Tateishi A. Experimental analysis of the spinal cord compressed by spinal metastasis. *Spine*. 1976;1989(14):1308-1315.
- Barth RF, Mi P, Yang W. Boron delivery agents for neutron capture therapy of cancer. *Cancer Commun (Lond)*. 2018;38:35.
- Porras JL, Pennington Z, Hung B, et al. Radiotherapy and surgical advances in the treatment of metastatic spine tumors: a narrative review. *World Neurosurg*. 2021;151:147-154.
- Sahgal A, Myrehaug SD, Siva S, et al. Stereotactic body radiotherapy versus conventional external beam radiotherapy in patients with painful spinal metastases: an open-label, multicentre, randomised, controlled, phase 2/3 trial. *Lancet Oncol*. 2021;22:1023-1033.
- Bilsky MH, Laufer I, Fourny DR, et al. Reliability analysis of the epidural spinal cord compression scale. *J Neurosurg Spine*. 2010;13:324-328.
- Ryu S, Rock J, Jain R, et al. Radiosurgical decompression of metastatic epidural compression. *Cancer*. 2010;116:2250-2257.
- Laufer I, Iorgulescu JB, Chapman T, et al. Local disease control for spinal metastases following "separation surgery" and adjuvant hypofractionated or high-dose single-fraction stereotactic

- radiosurgery: outcome analysis in 186 patients. *J Neurosurg Spine*. 2013;18:207-214.
40. Ling DC, Flickinger JC, Burton SA, et al. Long-term outcomes after stereotactic radiosurgery for spine metastases: radiation dose-response for late toxicity. *Int J Radiat Oncol Biol Phys*. 2018;101:602-609.
41. Hu N, Tanaka H, Yoshikawa S, et al. Development of a dose distribution shifter to fit inside the collimator of a boron neutron capture therapy irradiation system to treat superficial tumours. *Phys Med*. 2021;82:17-24.

How to cite this article: Fujikawa Y, Kawabata S, Tsujino K, et al. Boron neutron capture therapy delays the decline in neurological function in a mouse model of metastatic spinal tumors. *Cancer Sci*. 2024;115:2774-2785. doi:[10.1111/cas.16245](https://doi.org/10.1111/cas.16245)